

# SYNTHESIS OF VELOCITY REFERENCE CAM FUNCTIONS FOR SMOOTH OPERATION OF HIGH SPEED MECHANISMS

Robert M. C. Rayner and M. Necip Sahinkaya

*Department of Mechanical Engineering, University of Bath, Claverton Down, Bath BA2 7AY, U.K.*

**Keywords:** Cam function, mechanisms, identification, control, simulation.

**Abstract:** The purpose of the paper is to improve the dynamic performance of a mechanism used in a packaging machine in order to run the system at higher speeds with lower vibration and noise levels. A method of synthesising a velocity demand signal as a function of crank position (i.e. cam function) is demonstrated for a prototype mechanism and drive system. The method aims to minimise the peak to peak actuation torque requirements in order to minimise the vibration of the mechanism. First of all, experimental results are utilised to identify the drive system parameters. A dynamic simulation package is used to model the nonlinear dynamics of the mechanism. The model based synthesis of velocity reference cam functions is performed at increasing mechanism actuation speeds. The performance of the system using the proposed velocity demand cam function is compared with the conventional constant speed reference case at different running speeds.

## 1 INTRODUCTION

The dynamic performance requirements of modern machinery are constantly increasing in terms of operation speed and motional accuracy. To remain competitive, mechanisms need to run at ever higher speeds, with greater reliability and be manufactured at lower cost. To achieve this, machines use a combination of electrical control systems, servo systems and mechanisms to generate truly mechatronic solutions. At the core of most packaging machines are multi-linkage mechanisms, which interact with packaging materials and products. These mechanisms have highly nonlinear dynamic properties and introduce vibrations at high operating speeds.

Much work has been documented on optimum balancing of mechanisms in order to reduce the vibrations at high operating speeds, such as (Kochev, 2000; Lee and Cheng, 1984; Alici and Shirinzadeh, 2006) and others. This method involves the adding of balancing masses to the mechanism, which increases the weight and may not always be physically achievable due to factors such as space restrictions. Alternatively, a mechanism can be re-designed or re-synthesised by considering kinematic and dynamic cost functions (Conte et al., 1975; Kochev, 2000). Due to the large number of parameters, conventional optimisation techniques struggle. Many researchers tried to formulate new optimisation techniques, such as genetic algorithms (Connor et al., 1998; Cabr-

era et al., 2002; Laribi et al., 2004; Saxena, 2005), differential evolution (Price and Storn, 2006), artificial immune searching (Liu and Xiao, 2005), geometric centroid of precision positions technique (Shiakolas et al., 2005), and the time varying dimensions method (Hansen, 2002).

It has been stated in (Yuan and Rastegar, 2004) that vibrations experienced during high speed actuation are caused by harmonic content in the output motion. It has also been argued in (Rastegar and Yuan, 2002) that the amount of harmonic content present in the motion increases with the magnitude of the peak to peak torque required to generate the motion. Recently, an iterative method of synthesising a velocity command cam function has been introduced to reduce the peak to peak actuation torque (Sahinkaya et al., 2007). This method relies on the development of a computer model of the system. This model is based on experimental results and a simulation of the nonlinear dynamics of the mechanism. This paper extends the aforementioned work by synthesising optimised cam functions (i.e. velocity profile as a function of crank angle) to achieve higher output speeds than that discussed previously, and that used for the purpose of system identification. The use of shaped cam functions has demonstrated significant benefits in terms of reduced peak to peak torque requirements. This is a software based command shaping technique. No redesigning or re-synthesis of the mechanism is necessary.

## 2 SYSTEM DESCRIPTION AND MODELLING

The block diagram of the prototype system considered in this study is shown in Figure 1. The mechanism is a 6-bar mechanism called the *woodpecker* mechanism. The purpose of the mechanism is to push thin products into packaging held in a neighbouring hopper. The mechanism is driven by an Allen Bradley MPL 540K-MJ22AA servo controlled with an Allen Bradley Kinetix6000 drive unit via a belt drive with a 3:1 gear ratio. The drive unit is fundamentally a PI controller. The user can configure the drive unit and monitor the system in real-time using RSLogix5000 control software. The servomotor and the drive system is assumed to be a first order lag with a time constant of  $\tau$  and a gain  $K_m$ .

$$G_m = \frac{K_m}{1 + \tau s} \quad (1)$$

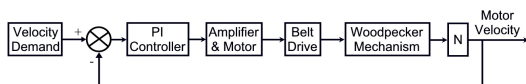


Figure 1: Block diagram of the overall system.

Before modelling the nonlinear dynamics of the woodpecker mechanism, experiments were carried out to identify the drive system parameters. It was possible to log the velocity demand, velocity output, acceleration output, position output, and motor torque. A step input velocity signal was used with different values of  $K_P$  and constant velocity demand. The integral gain  $K_I$  was set to zero during the identification process. To estimate the effective friction coefficient acting on the motor shaft, the steady state response over a single crank cycle was considered. By using the approximate constant speed section of the cycle, the friction coefficient  $b$  can be estimated from the following transfer function between the motor torque (the output of "Amplifier & Motor" block in Fig. 1) and the motor velocity:

$$\frac{T_{m,ss}}{\dot{\theta}_{m,ss}} = \frac{N^2}{b} \quad (2)$$

where  $T_{m,ss}$  and  $\dot{\theta}_{m,ss}$  are the average motor torque and motor speed respectively along the constant speed section of the steady state cycle, and  $N$  is the gear ratio, i.e.  $N = 3$ . This gave a representative friction coefficient of  $b = 0.255$ . In order to identify the motor/amplifier gain  $K_m$  and the effective rotor inertia, tests were repeated by replacing the woodpecker mechanism with a disk of known inertia. Thus the

steady state gain of the closed loop system can be written as:

$$\frac{\dot{\theta}_{m,ss}}{\dot{\theta}_{m,ref}} = \frac{N^2 K_m K_p}{b + N^2 K_m K_p} \quad (3)$$

By analysing the steady state system response, the motor/amplifier gain was estimated as  $K_m = 0.0883$ . Transient motor torque and motor velocity data were used to determine the effective inertia of motor shaft and associated pulleys acting on the crank shaft. Thus  $I_m = 0.0071 \text{ kgm}^2$ . Observation of the transient motor torque and the error signal suggested that the time constant  $\tau$  can be taken as zero. This may be due to a high-gain internal current feedback in the motor drive circuit.

The dynamic model for the woodpecker mechanism was built in Simulink by using *Dysim* (Hazerigg and Sahinkaya, 1984; Sahinkaya, 2004) simulation package. The mechanism consists of 6 links as shown in Figure 2. The physical data is given in Table 1. A CAD model of the mechanism was used to obtain these mass and inertia values and the position of the centre of gravity of each link and local coordinates of the connection points. The model was then tested using various demand speed and controller parameter combinations. For example, Fig. 3 shows the experimental and simulation results for a constant speed reference of 300 rpm with  $K_P = 20$  and  $K_I = 0$ .

The results showed an excellent match between the experimental and simulated responses for all the tests conducted with the prototype system. The high

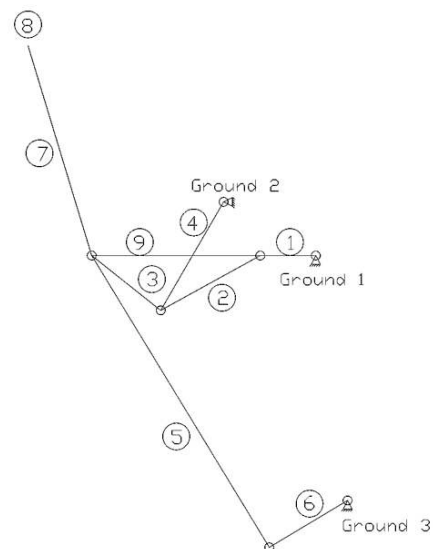


Figure 2: A schematic view of the woodpecker mechanism.

Table 1: Data for the Woodpecker mechanism.

Name	No	Length (mm)	Mass (kg)	Inertia (N·mm <sup>2</sup> )
Crank	1	62	0.927	901
Connector	2	127	0.310	1420
	3	103		
	9	188.3		
Upper pivot	4	144	0.414	1310
End-effector	8		0.174	380
Spine	5	348.86	0.482	10550
	7	245.19		
Lower pivot	6	102	0.123	290

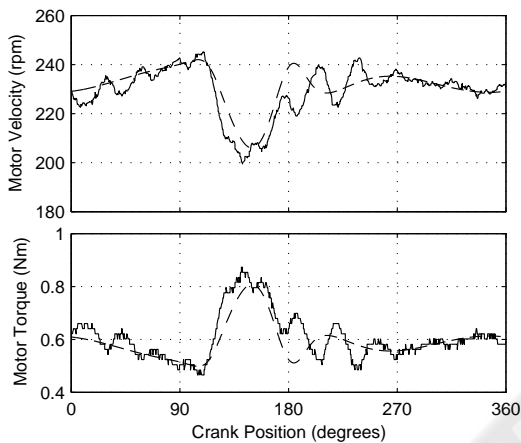


Figure 3: Simulated (dashed) and experimental (solid) steady state responses over one crank cycle.

frequency oscillations (of approximately at 15 Hz.) in the measured response were due to the belt dynamics, which were not included in the analysis. Particularly encouraging was the reproduction in the simulated results of the velocity trough and corresponding torque peak resulting from the nonlinear nature of the mechanism dynamics. The orbit of the end effector is shown in Figure 4. Normalised crank positions (unity normalised crank position corresponds to 360° crank angle) are shown on the orbit. The critical portion of the path is between normalised crank positions of 0.6 and 1.0, where the end-effector interacts with the product and product feeding mechanism.

### 3 OPTIMUM CAM PROFILE

The experimental results highlighted a potential problem when running the system at higher speeds. Of particular concern was the torque spike and trough on the return part of the end-effector orbit between crank positions 90 and 180 degrees. It has been shown elsewhere (Yuan and Rastegar, 2004) that harmonic content in the output motion induces vibra-

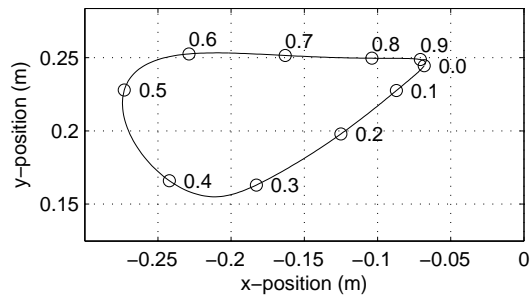


Figure 4: Orbit of the end-effector.

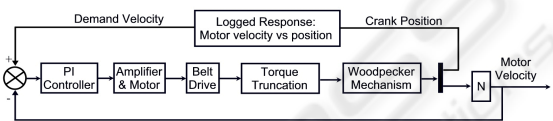


Figure 5: The process of optimising a velocity cam function.

tions and that the amount of harmonic content increases with the peak-to-peak magnitude of the actuation torque (Rastegar and Yuan, 2002). Therefore, the focus of the paper is to reduce the peak-to-peak drive torque through shaping the speed reference signal as a function of crank angle. The mechanisms will not be re-synthesised nor rebuilt. The method suggested in (Sahinkaya et al., 2007) utilises the model of the drive system estimated from experimental results. The procedure can be summarised as follows:

- Run the simulation of the overall system for a constant speed reference signal, and determine a narrow torque band from the steady state torque signal covering the approximate constant torque region.
- Run the simulation again with the same constant speed reference signal, but with saturation limits imposed on the drive torque. These limits are determined in (a). Then record the steady state output speed response over a single cycle of crank logged against crank position.
- Use the periodic output speed recorded in (b) as a velocity cam function and run the simulation without saturation limits to assess the performance of the system with this velocity cam function.

This process is shown in Figure 5 as a block diagram.

The above process is applied to the model of the prototype system to assess the benefit of the velocity cam function when the average running speed of the mechanism is increased from 100 rpm to 600 rpm. Due to the 3:1 gear ratio, this corresponds to

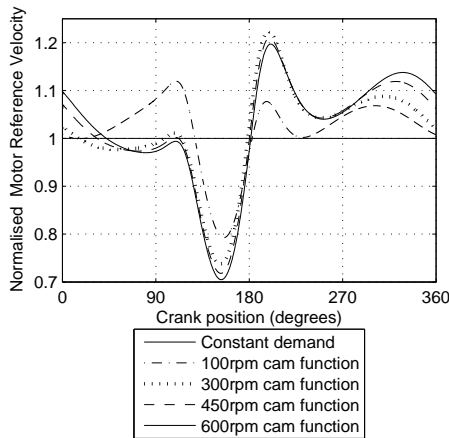


Figure 6: Velocity reference cam functions at different average crank speeds.

motor speeds from 300 rpm to 1800 rpm. The controller parameters are set to  $K_P = 20$  and  $K_I = 400$ . Figure 6 shows the synthesised cam functions at 300, 900, 1350, and 1800 rpm of the motor speed. For ease of comparison, the velocity reference signals are normalised by their corresponding constant speed values. Note that in each case the achieved average cyclic velocity of the mechanism corresponded closely to the demand velocity.

Figure 7 shows the corresponding steady state crank velocity output over a single crank cycle. Especially at higher speeds, the change in system response is minimal compared with the constant speed reference signal cases. Despite small variations in the output velocity profile, the use of the optimised cam function has significant benefits, greatly reducing the peak to peak drive torque requirements as shown in Figure 8. The benefit of the optimised cam function can be better appreciated from Figure 9, where the reduction in peak to peak torque variations are 99%, 80%, 78%, and 78% for the crank speeds of 100, 300, 450, and 600 rpm respectively.

Although it is not included in the optimisation process, the optimised velocity cam functions also reduce the maximum drive motor power requirements compared with the constant velocity signal case as shown in Figure 10.

#### 4 CONCLUSIONS

This paper demonstrates the benefit of using a velocity cam function as a velocity demand signal to reduce the peak to peak actuation torque of a servo driven mechanism. The drive system parameters were identified using experimental data, and then combined with

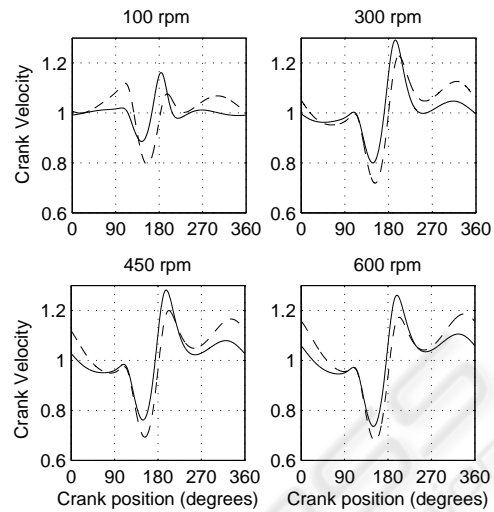


Figure 7: Normalised crank velocity output at different crank speeds (solid: constant reference, dashed: shaped reference).

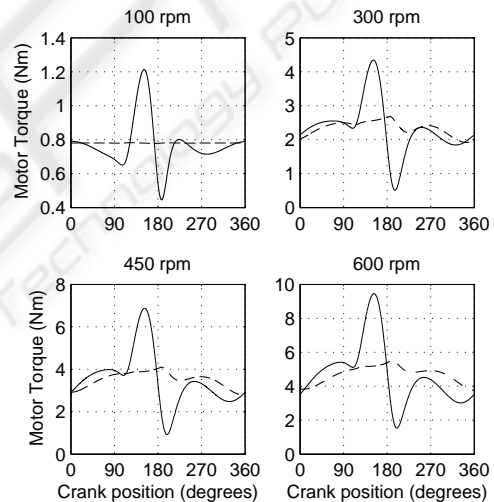


Figure 8: Drive torque at different crank speeds (solid: constant reference, dashed: shaped reference).

a nonlinear dynamic model of the mechanism. The identification was carried out at a crank speed of 100 rpm. The accuracy of the computer model has been verified using experimental results. Utilising the computer model, a three-stage synthesis of the velocity demand cam functions has been performed at much higher operational speeds up to 600 rpm. The results show that a reduction in peak to peak actuation torque of as much as 80% can be achieved at high speeds without significantly affecting the speed response of the system. Although no effort has been made to minimise the energy consumption, sizable reductions in the maximum motor power requirements have also been predicted.

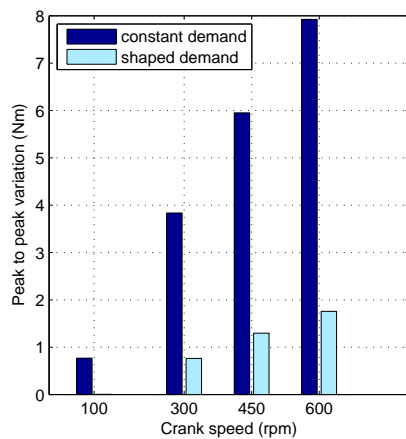


Figure 9: Peak to peak drive torque variations at different crank speeds.

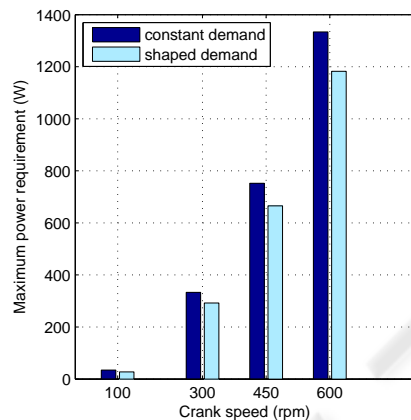


Figure 10: Maximum drive power requirements at different crank speeds.

## ACKNOWLEDGEMENTS

The authors acknowledge the support of the Engineering and Physical Sciences Research Council (EPSRC) of the U.K. and the industrial partner ITCM, Coventry, UK through the EPSRC Industrial Case Studentship Award Voucher No: 05002188.

## REFERENCES

Alici, G. and Shirinzadeh, B. (2006). Optimum dynamic balancing of planar parallel manipulators based on sensitivity analysis. *Mechanism and Machine Theory*, 41(12):1520–1532.

Cabrera, J. A., Simon, A., and Prado, M. (2002). Optimal synthesis of mechanisms with genetic algorithms. *Mechanism and Machine Theory*, 37(10):1165–1177.

Connor, A. M., Douglas, S. S., and Gilmartin, M. J. (1998). The use of harmonic information in the optimal syn-

thesis of mechanisms. *Journal of Engineering Design*, 9(3):239–249.

Conte, F. L., George, G. R., Mayne, R. W., and Sadler, J. P. (1975). Optimum mechanism design combining kinematic and dynamic-force considerations. *Journal of Engineering for Industry-Transactions of the ASME*, 97(2):662–670.

Hansen, J. M. (2002). Synthesis of mechanisms using time-varying dimensions. *Multibody System Dynamics*, 7(1):127–144.

Hazlerigg, A. D. G. and Sahinkaya, M. N. (1984). Computer aided design of non-linear systems. In *ACC 84 Conference*, pages 1498–1503.

Kochev, I. S. (2000). General theory of complete shaking moment balancing of planar linkages: a critical review. *Mechanism and Machine Theory*, 35(11):1501–1514.

Laribi, M. A., Mlika, A., Romdhane, L., and Zegloul, S. (2004). A combined genetic algorithm-fuzzy logic method (ga-fl) in mechanisms synthesis. *Mechanism and Machine Theory*, 39(7):717–735.

Lee, T. W. and Cheng, C. (1984). Optimum balancing of combined shaking force, shaking moment, and torque fluctuations in high-speed linkages. *Journal of Mechanisms Transmissions and Automation in Design-Transactions of the ASME*, 106(2):242–251.

Liu, Y. and Xiao, R. B. (2005). Optimal synthesis of mechanisms for path generation using refined numerical representation based model and ais based searching method. *Journal of Mechanical Design*, 127(4):688–691.

Price, K. and Storn, R. (2006). Differential evolution (DE), <http://www.icsi.berkeley.edu/storn/code.html>. Electronic Citation.

Rastegar, T. and Yuan, L. (2002). A systematic method for kinematics synthesis of high-speed mechanisms with optimally integrated smart materials. *Journal of Mechanical Design*, 124(1):14–20.

Sahinkaya, M. N. (2004). Inverse dynamic analysis of multiphysics systems. *Proceedings of the Institution of Mechanical Engineers Part I- Journal of Systems and Control Engineering*, 218(11):13–26.

Sahinkaya, M. N., Rayner, R. M. C., Vernon, G., Shirley, G., and Aggarwal, R. K. (2007). Synthesis of demand signals for high speed operation of a packaging mechanism. In *ASME International Design Engineering Technical Conferences & Computers and Information in Engineering Conference (IDETC)*.

Saxena, A. (2005). Synthesis of compliant mechanisms for path generation using genetic algorithm. *Journal of Mechanical Design*, 127(4):745–752.

Shiakolas, P. S., Koladiya, D., and Kebrle, J. (2005). On the optimum synthesis of six-bar linkages using differential evolution and the geometric centroid of precision positions technique. *Mechanism and Machine Theory*, 40(3):319–335.

Yuan, L. F. and Rastegar, J. S. (2004). Kinematics synthesis of linkage mechanisms with cam integrated joints for controlled harmonic content of the output motion. *Journal of Mechanical Design*, 126(1):135–142.